Investigation of hydrodynamic parameters distribution in heat exchange tubes of falling film evaporator

Cite as: AIP Conference Proceedings **2388**, 020006 (2021); https://doi.org/10.1063/5.0068408
Published Online: 19 November 2021

V. N. Gushshamova, A. P. Khomyakov, S. V. Mordanov, et al.

Investigation of Hydrodynamic Parameters Distribution in Heat Exchange Tubes of Falling Film Evaporator

V.N. Gushshamova[a)], A.P. Khomyakov, S.V. Mordanov, T.V. Khomyakova

Ural Federal University, 19, Mira str., 620002, Yekaterinburg, Russia.

[a)]Corresponding author: 89126634949@yandex.ru

Abstract. The purpose of this work is investigation of changes in hydrodynamic parameters (absolute pressure, mass flow rates of solution and secondary steam, secondary steam velocity, solution irrigation density, and pressure loss) along the length of the heat exchange tube of a vertical falling film evaporator. The obtained data of the distribution of hydrodynamic parameters were used in the design of falling film evaporators.

INTRODUCTION

Falling film evaporators are widely used in various industries. This application is due to the high intensity of heat exchange, high performance with relatively small volumes of the apparatus itself and insignificant production area [1-3]. Experimental studies of the hydrodynamics of the irrigation liquid film in horizontal film evaporators are presented in literature [4, 5].

The purpose of this work is investigation of changes in hydrodynamic parameters (absolute pressure, mass flow rates of solution and secondary steam, secondary steam velocity, solution irrigation density, and pressure loss) along the length of the heat exchange tube of a vertical falling film evaporator.

DESCRIPTION OF THE INVESTIGATION

Study of hydrodynamics was carried out by means of a mathematical numerical simulation for the falling film evaporator, equipped with heat exchange tube (with diameter Ø38x2 mm and length L=7 m). Data were obtained from the length of the heat exchange tube with step ΔL=0.1 m.

For the numerical simulation, we used the mathematical model based on the momentum conservation equation in terms of the pressure changes due to the steam and liquid film frictional and dynamical pressure changes, local hydraulic resistances, gravitation, and steam and liquid physical properties on the saturation line changing with the absolute pressure decreasing. The physical properties of the solution and steam were described using experimental data approximation equations with the approximation error of no more than 2-3 %. The solution thermal depressions and boiling temperatures were calculated using the ebullioscopic method.

Main technological parameters of the device operation:

1. Volume flow rate of the initial solution: 50 l/h, 100 l/h, 150 l/h;
2. Effective temperature difference – 15 °C;
3. Temperature of the initial solution – 70 °C;
4. Boiling point of the initial solution – 70 °C;
5. The heat transfer coefficient was assumed to be constant over the entire length of the heat exchange tube, equal to 2000 W/(m2·K).

RESULTS OF THE STUDY

The absolute pressure changes along the length of the heat exchange tube of the falling film evaporator at volume flow rates of the initial solution 50 l/h, 100 l/h, 150 l/h are shown in figure 1. At volume flow rates of 50 l/h and 100 l/h, the absolute pressure varies along the length of the tube from 31000 Pa to 28589 Pa and from 31000 Pa to 27532 Pa, respectively. When the volume flow rate of the initial solution increases to 150 l/h, the absolute pressure changes from 31000 Pa to 26519 Pa along the length of the heat exchange tube.

Modern Synthetic Methodologies for Creating Drugs and Functional Materials (MOSM2020)
AIP Conf. Proc. 2388, 020006-1–020006-4; https://doi.org/10.1063/5.0068408
Published by AIP Publishing. 978-0-7354-4142-2/$30.00

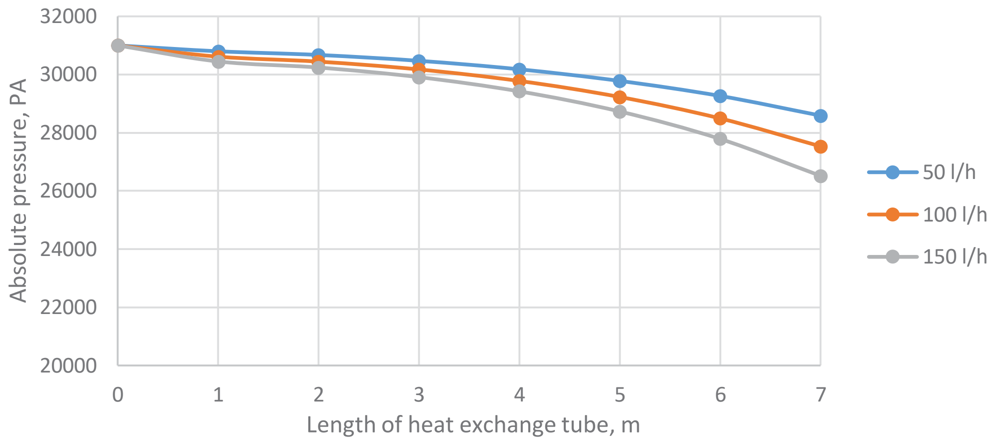

FIGURE 1. Distributions in absolute pressure in the tube space of the falling film evaporator

It is established that an increase in the volume flow rate of the initial solution leads to an increase in hydraulic resistance.

Figure 2 shows distributions of the mass flow rates of the solution along the heat exchange tube length. It is found that for all the considered volume flow rates of the initial solution, the amount of solution along the length of the tube decreases and changes almost linearly.

Distributions of the mass flow rates of secondary steam along the heat exchange tube length at different flow rates of the initial solution are shown in figure 3. It is established that an increase in the volume flow rate of the initial solution leads to an increase in the mass flow rate of secondary steam. The change is linear for the mass flow rate of secondary steam along the heat exchange tube length.

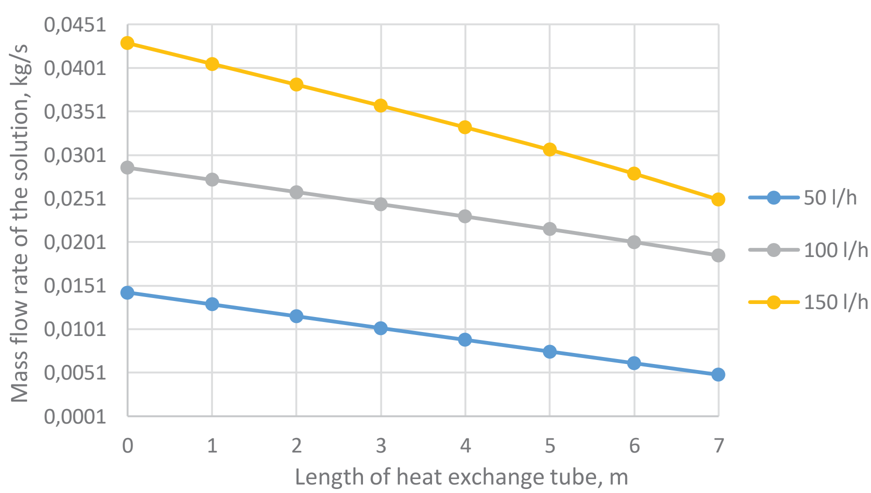

FIGURE 2. Distributions of the mass flow rate of the solution in the tube space of the film evaporator

The distribution of the volume density of irrigation along the length of the heat exchange tube of the falling film evaporator is shown in figure 4. The volume density of irrigation at the volume flow rate of the initial solution of 50 l/h varies from 0.00013 m3/(s·m) to 0.00001 m3/(s·m). When the volume flow rate of the initial solution is 100 l/h, it changes from 0.00026 m3/(s·m) to 0.00017 m3/(s·m). When the volume flow rate of the initial solution is 150 l/h, it changes from 0.0004 m3/(s·m) to 0.00023 m3/(s·m). The change in the volume density of irrigation with an increase in the volume flow of the initial solution is almost linear.

Figure 5 shows the distribution of the secondary steam velocity along the length of the heat exchange tube. At the following volume flow rates of the initial solution, the velocity of secondary steam at the outlet of the heat exchange tube reaches the values:

- for flow rate 50 l/h – 56 m/s;
- for flow rate 100 l/h – 62.7 m/s;
- for flow rate 150 l/h – 67.2 m/s.

It was found that an increase in the volume flow rate of the initial solution leads to an increase in velocity of secondary steam.

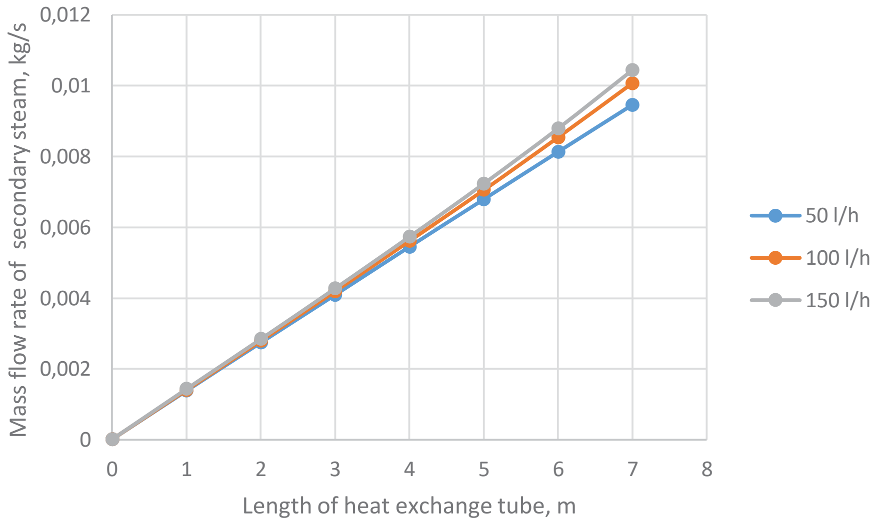

FIGURE 3. Distributions of the mass flow rate of secondary steam in the tube space of the film evaporator

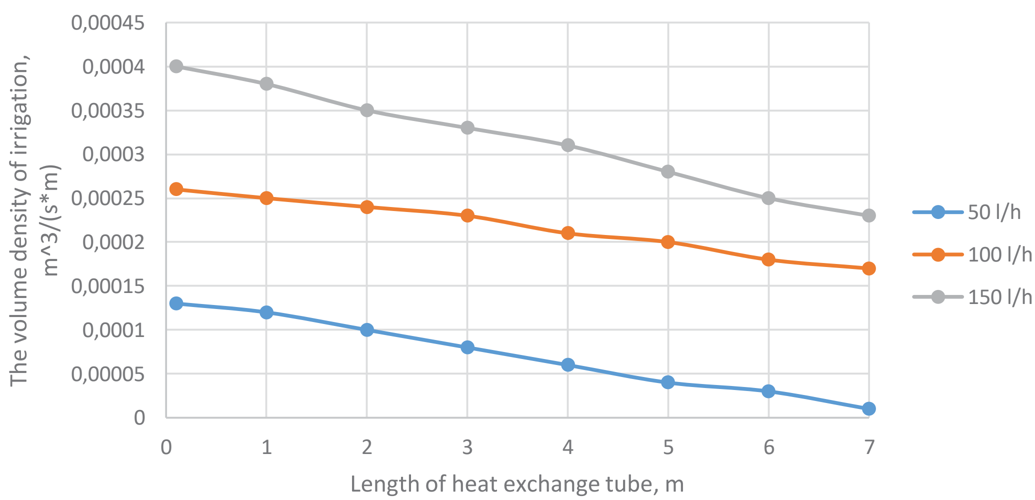

FIGURE 4. Distributions of volume density irrigation along the length of the heat exchange tube

Distributions of pressure losses along the length of the tube for each test mode of the initial solution are shown in figure 6. When the initial solution is consumed at 50 l/h, the pressure loss along the length of the heat exchange tube varies from 134 Pa to 2411 Pa. At the flow rate of the initial solution of 100 l/h, the pressure loss along the length of the heat exchange tube varies from 297 Pa to 3468 Pa. At the flow rate of the initial solution of 150 l/h, the pressure loss along the length of the heat exchange tube varies from 431 Pa to 4481 Pa. The local hydraulic resistance at the inlet to the tube explains the pressure change in the initial section of the heat exchange tube. Pressure losses along the length of the heat exchange tube occur due to changes in the dynamical pressure, due to the friction of the solution film against the tube wall, and due to the friction of steam against the solution film. The graph shows that an increase in the volume flow of the initial solution leads to an increase in the values of pressure losses along the length of the heat exchange tube.

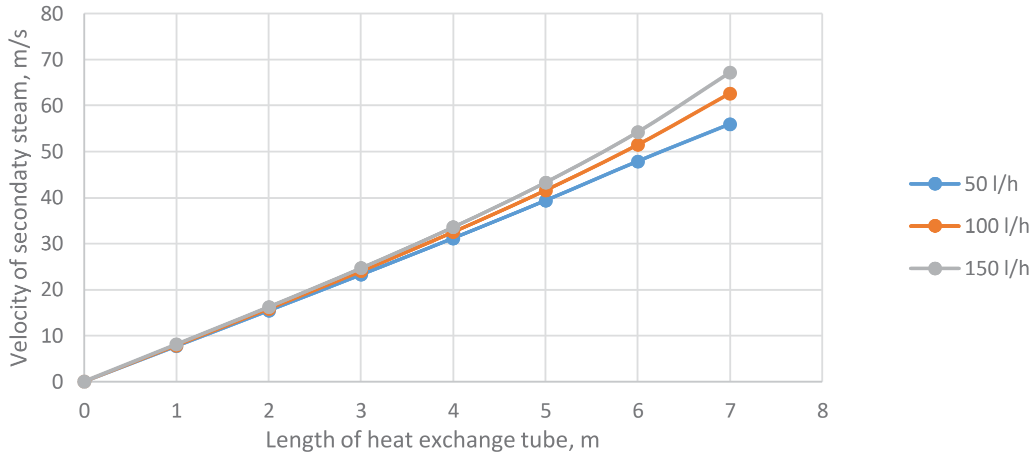

FIGURE 5. Distributions of velocities of secondary steam along the length of the heat exchange tube

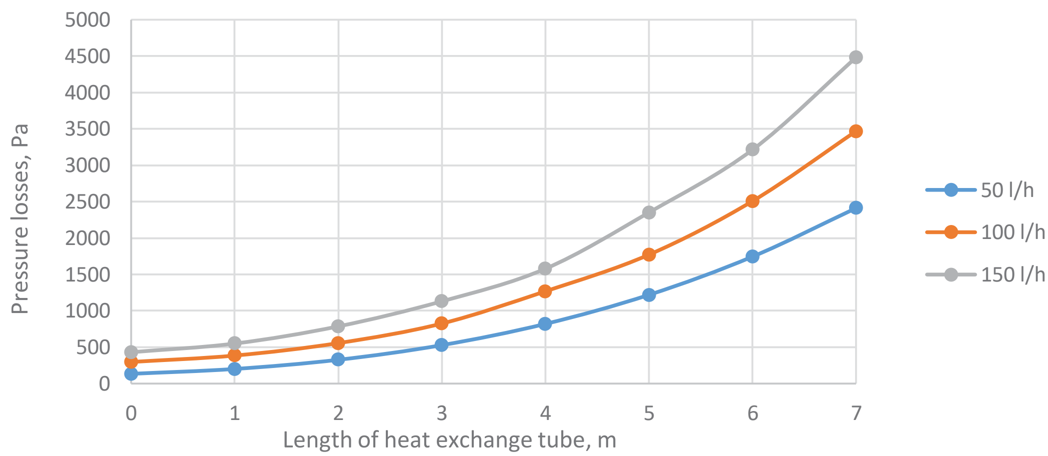

FIGURE 6. Distributions of hydraulic resistance along the length of the heat exchange tube

CONCLUSION

In our research, we have studied changes of the hydrodynamic parameters of a two-phase flow along the length of the heat exchange tube of the falling film evaporator. The research was carried out using mathematical numerical modeling.

Distributions at the length of the heat exchange tube are obtained: absolute pressure, secondary steam velocity, liquid phase irrigation density, mass flow rates of the solution and secondary steam, and pressure losses. The obtained data of the distribution of hydrodynamic parameters were used in the design of falling film evaporators.

REFERENCES

1. F.C. Standiford, Chemical Engineering Progress **70**, 157 (1974).
2. J.G. Moore, Chemical Engineering Progress **59**, 87-92 (1963).
3. J.R. Sinek, E.H. Young, Chemical Engineering Progress **58**, 74-80 (1962).
4. Q. Wang, M. Li, W. Xu, L. Yao, X. Li, D. Su, P. Wang, International Journal of Heat and Mass Transfer **163**, (2020).
5. E. Aursanda and T. Ytrehus, International Journal of Multiphase Flow **116**, 67-79 (2019).